Branching Effects in Physical Gelation of Atactic Polystyrene

Noureddine Lehsaini, Nawel Boudenne, Jean Georges Zilliox, and Dominique Sarazin*

Institut Charles Sadron, Université Louis Pasteur, 6 rue Boussingault, 67083 Strasbourg Cedex, France

Received October 13, 1993; Revised Manuscript Received April 21, 1994•

ABSTRACT: In this paper we give new results on the physical gelation of atactic polystyrene–carbon disulfide (CS_2) solutions in relation to the structure of the chains. We demonstrate here the starlike effect on the onset of gelation supported by well-improved techniques such as the ball-drop method, differential scanning calorimetry, measurements of the static modulus, and oscillatory rheometry. The sol–gel phase diagrams show that the increase of the degree of branching has a noticeable impact on gel formation but with approximately constant melting enthalpy. The chemical junctions between branches in the star molecules result in an increase of the gelation temperature with respect to linear chains of equal concentration and overall molecular weight and in a decrease in the gel modulus at a given concentration.

I. Introduction

Physical gels are obtained from semidilute solutions of atactic polystyrene by cooling at a temperature which depends on the concentration and molecular weight of the polymer and on the nature of the solvent.[1-12] The polymer tacticity is also an important feature in the formation mechanism of chain junctions.[3,4,6,7]

The relatively high temperature of gelation observed in carbon disulfide (CS_2) explains the large number of studies devoted to the system aPS–CS_2, using various methods such as rheology, calorimetry, and light scattering. It was proposed that gelation of aPS originates from a liquid–liquid demixing.[5,8,9] Such a model implies a relation between the thermodynamic quality of the solvent and the gelation temperature, the better solvent giving the lowest gelation temperature. This is consistent with the results of a comparison of the behavior of *cis*- and *trans*-decalin solutions of aPS.[9] Viscosity measurements show that it is unambiguously a good solvent in the temperature range of the sol–gel transition. It turns out that gelation is not directly related to the thermodynamic solvent quality and is not the prerogative of poor solvents.

The overall picture which has emerged is that gelation is due to intermolecular associations of chain segments in complex crystals including syndiotactic segments and solvent molecules. This has been deduced from calorimetric measurements performed with aPS samples of various tacticities in different solvents.[7] A recent systematic study of the aPS–carbon disulfide system by depolarized light scattering (H_v)[13] has demonstrated that a part of the chains is stiffened upon gelation. The concentration dependence of the viscoelastic properties of aPS–CS_2 semidilute solutions is consistent with the theoretical predictions.[14] At the gelation point, an abrupt change in the plateau modulus G_N is observed but the exponent of its concentration dependence is almost unmodified. Phase diagrams and rheological properties of the gel begin to be well understood for linear polystyrene, and it was interesting to check the influence of chemical cross-links on the gelation phenomenon.

Accordingly, we have prepared two sets of star atactic polystyrenes with three and four branches, respectively, using the advantages of anionic polymerization, which provides polymers of well-controlled degree of branching and molecular weight.

This paper presents a systematic study of the gelation temperature, the Young's modulus E, and the dynamic storage and loss moduli, $G'(\omega)$ and $G''(\omega)$. The results show that the plateau modulus of the branched atactic polystyrene has a concentration dependence close to the theoretical law $c^{2.25}$ and that the gelation temperature increases with increasing number of branches.

II. Experimental Section

A. Polymer Synthesis and Characterization. We prepared star-shaped atactic polystyrenes according to the method described by Herz et al.[15] The process is based upon the termination reaction of polystyrene carbanions with multifunctional electrophilic reagents. 2,4,6-Tris(allyloxy)-1,3,5-triazine (TT) and 1,1,4,4-tetraphenyl-1,4-bis(4,6-bis(allyloxy)-1,3,5-triazin-2-yl)butane (DT) were used to generate star-shaped PS with three branches (PS*) and four branches (PSD*), respectively.

Solvents and Reagents. Tetrahydrofuran (THF) (SDS, 99.5%) was treated with sodium benzophenone complex after distillation over sodium wire. The dry solvent recovered by distillation from the organometallic was stored, like all of the reagents used, in capped burettes under a slight argon pressure. Styrene (Merck, 99%) was distilled twice over sodium wire under reduced pressure just before use. TT (Degussa) was recrystallized from heptane and vacuum distilled. DT was obtained reacting tetraphenyldiiodobutane (dimerization product of 1,1-diphenylethylene by sodium in THF) with an excess of TT. The product was recovered by crystallization.

Polymerization Procedure. Anionic polymerization of styrene, initiated by (1-phenylethyl)potassium, was carried out in THF at low temperature (−70 °C) in a perfectly closed glass reactor purged before use by heating under vacuum and by vacuum–argon cycles. After neutralization of the traces of the electrophilic impurities with a few drops of the initiator solution (until persistence of a light red color) and addition of the required amount of initiator, the styrene was introduced dropwise.

As the polymerization reached completion, a sample was taken off under argon and deactivated by methanol, thus giving access to the molecular characteristics of the precursor PS "branch".

The "ramification" reaction of the precursor monocarbanionic PS "branches" was achieved by reacting them with a stoichiometric amount of the three or four allyloxy functions carried by the TT or DT molecule, respectively. The polymers were precipitated, washed in methanol, and dried at 50 °C under reduced pressure. A representation of the structures of the star-shaped polystyrenes is given in Scheme 1.

Characterization. (1) Gel Chromatography. The linear precursor PS and star-shaped PS* and PSD* polystyrenes were characterized by size exclusion chromatography (SEC) in THF. The apparatus consists of two concentration detectors, a refrac-

* To whom all correspondence should be sent.

• Abstract published in *Advance ACS Abstracts*, June 15, 1994.

0024-9297/94/2227-4353$04.50/0

Table 1. Weight-Average Molecular Weight (M_w) and Polydispersity Index (M_w/M_n) Obtained by Size Exclusion Chromatography in Tetrahydrofuran with either UV or Refractometric Detection

	UV				refractometer			
	M_n	M_w	M_w/M_n	M_b/M_l	M_n	M_w	M_w/M_n	M_b/M_l
PS	6 100	6 330	1.03	$P_n = 2.8$	6 120	6 330	1.03	$P_n = 2.9$
PS*I	17 100	18 200	1.07	$P_w = 2.9$	17 600	18 200	1.04	$P_w = 2.9$
PS	12 200	12 600	1.03	$P_n = 2.5$	12 000	12 600	1.04	$P_n = 2.6$
PS*II	30 300	34 900	1.15	$P_2 = 2.8$	31 200	34 900	1.12	$P_w = 2.8$
PS	56 900	58 100	1.02	$P_n = 2.3$	56 800	58 100	1.02	$P_n = 2.4$
PS*III	131 000	152 000	1.16	$P_w = 2.6$	132 000	152 000	1.15	$P_w = 2.6$
PS	117 000	121 000	1.04	$P_n = 1.5$	116 000	121 000	1.05	$P_n = 1.5$
PS*IV	169 000	259 000	1.54	$P_w = 2.1$	173 000	259 000	1.52	$P_w = 2.2$
PSD*1	109 000	129 000	1.26	$P_n = 4$				
PSD*2	209 000	300 000	1.5	$P_w = 4$				

Scheme 1

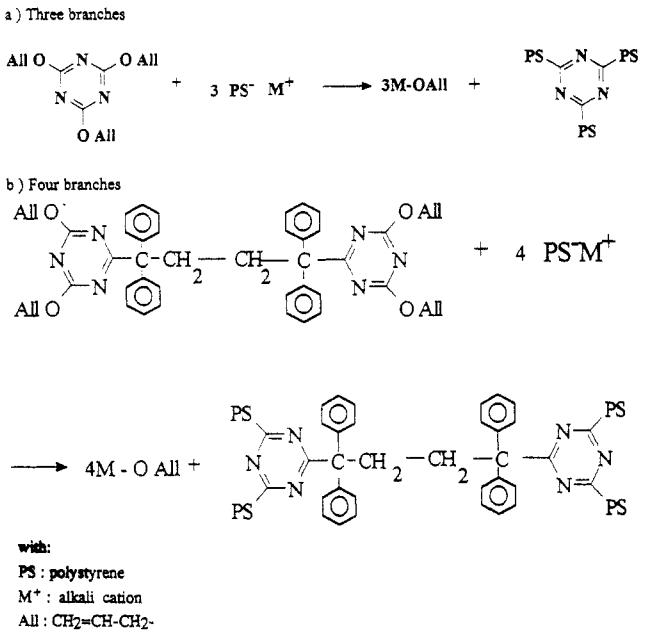

tometer, a spectrophotometer, and a low-angle laser light scattering apparatus. This equipment allows the determination of the weight-average (M_w) and number-average (M_n) molecular weights without any previous calibration procedure. The results obtained with the two concentration detectors are reported in Table 1. The ratios p_n and p_w between the weight- and number-average molecular weights of the three-branch star polymers and the linear precursors are close to 3 for samples PS*I to PS*III. This ascertains the stoichiometric reaction of the trifunctionalization, but the result is rather poor for PS*IV.

(2) NMR Spectroscopy. Carbon-13 NMR spectra were measured using a Bruker spectrometer equipped with a PFT-100 Fourier transform system operating at 50 MHz and were observed by an external locked field sweep in the absorption mode on solutions of 50% of polymer in chloroform. Measurements were made at 50 °C on samples in 8-mm glass tubes. All ^{13}C chemical shifts are expressed in parts per million with respect to the chloroform peak, positive values corresponding to upfield shifts and vice versa.

In Figure 1 are shown carbon-13 NMR spectra of samples PS*IV and PSD*2 in chloroform. Assignment of individual peaks to corresponding carbons in the polymer was carried out by comparison with the carbon-13 spectrum of polystyrene in tetrachloroethylene at 120 °C.[16]

B. Physicochemical Methods. Ball-Drop Method. The gelation temperatures were obtained by the ball-drop method as described by Takahashi et al.[17] Known quantities of polymer and solvent were introduced into a glass tube with a steel ball after careful drying and handling in a dry glovebox. The system was then sealed and kept at room temperature for 1 week before further experimentation. The observation of the ball drop starts after the temperature of the thermostating bath is increased. Initially, the steel ball rolls freely on the surface; then it begins to fall at the temperature of gel melting (T_{gel}).

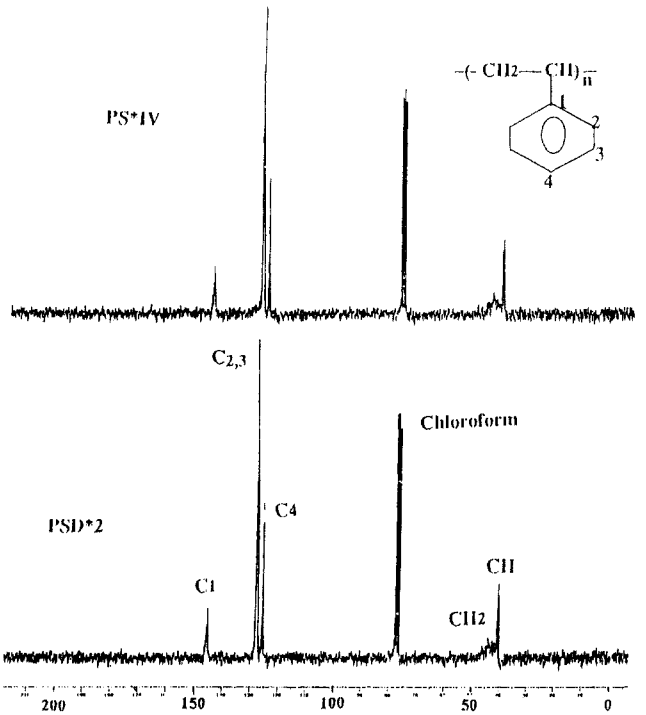

Figure 1. ^{13}C NMR spectra of star polystyrenes observed at 50 MHz: PS*IV and PSD*2 in 50% (w/v) solution in chloroform-*d* at 50 °C.

Differential Scanning Calorimetry (DSC). A Perkin-Elmer DSC microcalorimeter equipped with a Thermal Analysis Data Station (TADS) was employed. The handling was carried out in a dry glovebox under a slight dry-nitrogen flow till the end of the pan sealing. A desired quantity of vitrified PS* was introduced into a weighed volatile sample pan, and an estimated volume of CS_2 was added drop by drop. The pans were annealed for several days at 42 °C and then for at least 8 days at room temperature to ensure a thorough homogenization. The weight of each pan was measured prior to taking any data to determine the concentration of the system (in g/mL) and after the thermal scans. Some DSC measurements were repeated a month later to ascertain the reproducibility of the DSC traces. These controls have shown the preparation procedure to be quite satisfactory. The heating rate was set at 20 °C/min. Moreover, to measure with sufficient accuracy and reliability the very low melting enthalpy (ΔH_m) values as well as to detect broad melting endotherms, a good straight base line is required. This was obtained after several scans on an empty pan to minimize the noise due to the apparatus mainly at the lowest temperature.

Young's Modulus Measurements. The Young's modulus E was measured with a home-built apparatus working in uniaxial compression. It includes a HBM (Hottinger Baldwin Messtechniк (GmbH) amplifier coupled to a force transducer connected to a measurement Teflon cylinder (diameter $\phi_c = 15$ mm, height = 20 mm). The force transducer can move the cylinder to the gel surface by micrometric steps with the help of a microcontrol translator. In fact, this type of device is well adapted to the case of chemically cross-linked gels whose pieces of well-defined

geometry can be prepared. One generally utilizes cylinders of diameter equal to that of the Teflon cylinder, and they are immersed in the solvent for the measurements. This is much more difficult to realize with thermoreversible gels. The solutions or gels were confined in a cell of diameter larger than ϕ_c. By studying the elastic moduli of chemically cross-linked polyacrylamide gels swollen in water, we found that the wall effects for confined gels can be minimized if $\phi_c > 26$ mm. A cylindrical glass cell of $\phi_t = 26$ mm and height $h = 8$ mm was used in this work. This cell was put into a well-adjusted double-wall brass cylinder thermostated at ±1 °C by circulating 2-propanol from a Haake cryostat. To avoid problems arising from water condensation at the surface of the gel, all mechanical parts of the device were put in a glovebox under a dry-nitrogen flow.

A typical measurement was conducted as follows: the PS–CS_2 solution was introduced into the glass cell, which was immediately closed to avoid CS_2 evaporation. Then the temperature was lowered to −25 °C (this temperature is lower than the sol–gel transition temperature (T_{gel}) of all the samples studied). The nitrogen flow was set and stopped during measurements. Then the measurements were made by raising the temperature by steps of 5 °C, the solution being kept at each temperature for 1.30 h. The statistical theory of rubber elasticity[18,19] gives the simple following form for the stress–strain equation:

$$\sigma = (E/3)(\lambda - \lambda^{-2}) \tag{1}$$

λ is related to the uniaxial deformation γ_{uniax} by

$$\lambda = 1 + \gamma_{uniax} \tag{2}$$

For small deformations ($\gamma_{uniax} < 10\%$), eq 1 is reduced to

$$\sigma = E\gamma_{uniax} \tag{3}$$

In each experiment, the value of E is deduced from the slope of the linear part of the plot of $\sigma = f(\gamma_{uniax})$.

Rheological Measurements. The dynamic storage and loss moduli $G'(\omega)$ and $G''(\omega)$ were measured with a stress-controlled rheometer (Carrimed CSL 100) equipped with a cone cylinder geometry as a function of frequency ($10^{-2} < \omega < 62.8$ s^{-1}). $G'(\omega)$ and $G''(\omega)$ are evaluated from the data with a shear γ magnitude less than 0.1 to remain in a linear range. The device can be thermostated by 2-propanol circulation at ±1 °C. Water condensation on the metallic parts was avoided with a dry-nitrogen flow. Due to the immiscibility of the silicone oil in CS_2, a thin layer of low-viscosity silicone oil is put at the surface of the solvent or the solution to be measured in order to prevent evaporation. Therefore, the oil stays away from the gel–cylinder surfaces and cannot perturb the measurements. Moreover, the measurements made just before and after the deposit of the oil layer are quite similar. The concentration was found to vary by less than 2% during all measurement cycles. All measurements were performed at $T = -25$ °C ($T < T_{gel}$).

In an elastic incompressible material, the relation between the shear modulus G_N and the Young's modulus E is

$$E = 3G_N \tag{4}$$

Viscosity Measurements. Viscosity measurements were performed at 25 ± 0.1 °C on an automatic water-thermostated jacket capillary viscosimeter.[20] The capillary diameter was ϕ = 0.46 mm, and the volume was 4 mL. Before measurements, the apparatus was carefully rinsed with well-dried CS_2 to eliminate water absorbed on the glass.

In this permanent Poiseuille type rheometer the shear rate is around 1000 s^{-1} for dilute solutions. We checked the Newtonian behavior of the grafted polystrene dilute solution by using a low-shear Couette type rheometer (LS30, Contraves). No shear rate dependence was found in the range of molecular weights studied here.

III. Results

A. Viscosity of the Dilute Solutions. The measurement of the intrinsic viscosity [η] can constitute a control

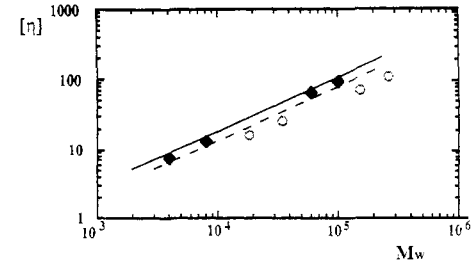

Figure 2. Variation of the intrinsic viscosity [η] (mL/g) as a function of molecular weight: PS* in CS_2 (○) compared with PS/CS_2 (◆) and the calculated curve (9) (– – –).

of the star structure and a measure of the number of branches since the molecular dimensions of branched macromolecules are well known to be lower than those of their linear homologs. Zimm and Stockmayer[21] have defined a structure parameter g as the ratio

$$g = R_{gb}^2/R_{gl}^2 \tag{5}$$

where R_{gb} and R_{gl} are the radii of gyration of the branched and linear polymers, respectively. For a starlike polymer, a relation between g and the number of branches p has been proposed by Stockmayer and Fixman:[22]

$$g = \frac{3p - 2}{p^2} \tag{6}$$

For a three-branch star, $g = 0.778$.

Zimm and Kilb[23] have shown that due to the competing effects of branching on the static dimensions and hydrodynamic interaction, the ratio of the intrinsic viscosities of a branched chain to a linear chain of equal molecular weight at the Θ point is given by

$$[\eta]_b/[\eta]_l \approx g^{1/2} \tag{7}$$

This formula is valid for a good solvent if the swelling ratio α of branched and linear chains is approximately the same, as shown by Strazielle et al.[15]

From the Mark–Houwink law obtained by Gan et al. for linear aPS in CS_2 at 25 °C

$$[\eta]_l = 7 \times 10^{-3} M^{0.76\pm0.02} \quad \text{(mL/g)} \tag{8}$$

the following molecular dependence of $[\eta]_b$ can be predicted from relations 6 and 7 for three-branch aPS in the same solvent and temperature:

$$[\eta]_b = 6.14 \times 10^{-3} M^{0.76\pm0.02} \quad \text{(mL/g)} \tag{9}$$

Relations 8 and 9 are reported in Figure 2 together with the experimental results for the three-branch PS*. The experimental values lie slightly above the calculated curve (9). This can be explained by an average number of branches less then 3 (see Table 1).

B. Phase Diagrams. Figure 3 shows the phase diagrams of the three-branch PS*/CS_2 system determined from the ball-drop method[17] for different molecular weights. T_{gel} is an increasing function of molecular weight at a given concentration. Moreover, for each sample, T_{gel} is a monotonically increasing function of concentration.

The sol–gel transition curves of linear PS and stars PS* and PSD* of approximately the same molecular weight are compared in Figure 4. A significant increase of T_{gel} with the number of branches is observed: as an example, at $c = 0.3$ g/mL, T_{gel} passes from 1 °C for the linear sample

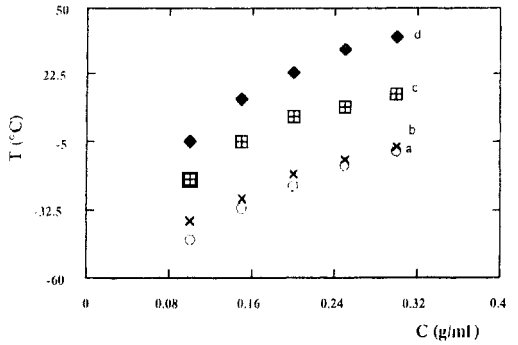

Figure 3. Variation of T_{gel} as a function of concentration c (g/mL) for PS* samples of different molecular weights: (○) PS*I; (×) PS*II; (⊞) PS*III; (◆) PS*IV.

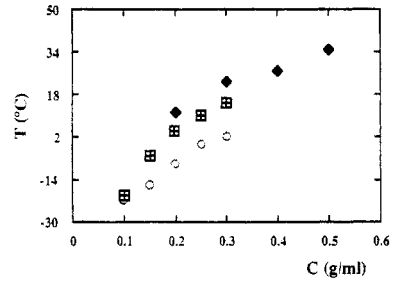

Figure 4. Variation of T_{gel} as a function of concentration c and of number of branches for PS of approximately the same molecular weight: (⊞) PS*III(M_w=152000); (◆) PSD*-(M_w=129000); (○) $PS_{(linear)}$(M_w=180000).

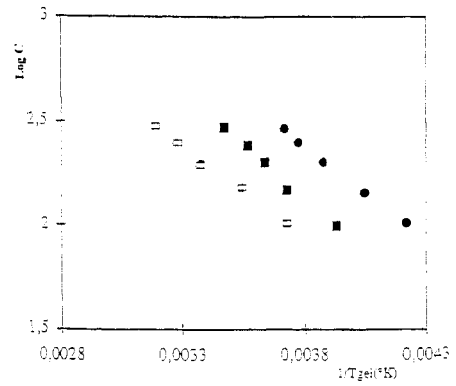

Figure 5. Dependence of $1/T_{gel}$ on log c (g/mL) for PS* samples of different molecular weights: (●) PS*I; (■) PS*II; (□) PS*III.

to 16 and 22 °C for the three- and four-branch star PS. This means that the chemical junctions stabilize the gel phase.

For linear polymers, the concentration and molecular weight dependence of T_{gel} has been analyzed according to the relation derived by Ferry and Eldridge:[24]

$$\log c = \frac{\Delta H_m}{2.3RT_{gel}} + f(M_w) \qquad (10)$$

where T_{gel} is the melting temperature of the gel and ΔH_m is the enthalpy of formation of the segment–segment association. Plots of log c = f($1/T_{gel}$) are drawn in Figure 5. The ΔH_m values are similar for branched and linear aPS (see Table 2).

C. Differential Scanning Calorimetry (DSC). Figure 6 displays DSC traces recorded under heating for the PSD*1/CS_2 system of various concentrations. An enthalpy of gel formation can be evidenced which clearly confirms previous findings by Gan et al.[3] (Figure 7).

Figure 8a shows the phase diagram obtained by DSC for a four-branch star (PSD*1/CS_2). The onset and end

Table 2. Comparison of Gelation Enthalpies of Linear and Branched Polymers

polymer	ΔH (kJ/mol) obtained by the slope of log c = f($1/T$) (Figure 5)
PS(linear)(M_w=2×10^5)	24.7
PS(linear)(M_w=4.1×10^5)	26.4
PS(linear)(M_w=6.7×10^5)	28
PS*I(M_w=18200)	18.1
PS*II(M_w=34900)	22.5
PS*III(M_w=152000)	27.3

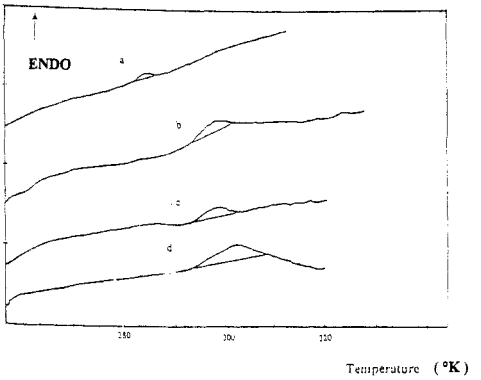

Figure 6. DSC thermograms for PSD*1 in CS_2 at different polymer concentrations: (a) 0.23, (b) 0.32, (c) 0.41, and (d) 0.54 g/mL.

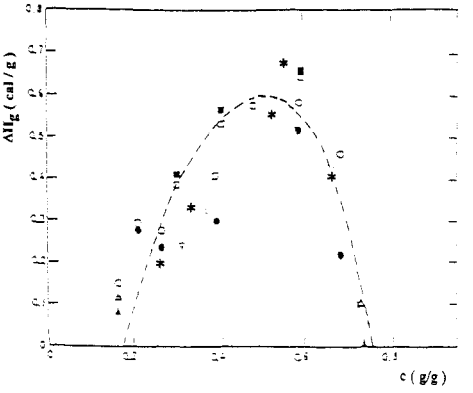

Figure 7. Enthalpies of fusion for different molecular weights (ΔH in cal/g). (*) PSD*1, together with the experimental results for linear PS/CS_2 of Gan et al.[3] (The curve indicates that ΔH is independent of molecular weight.)

of the peak have been reported to give an idea of the width of the peak. For moderately concentrated solutions, T_{gel} as determined by the maximum of the melting endotherm corresponds, within a few degrees, to T_{gel} as measured by the ball-drop method (Figure 8b). This indicates that the DSC endotherm is unambiguously with the sol–gel transition.

D. Young's Modulus Measurements. A typical variation of σ with γ for a gel of sample PS*III is depicted in Figure 9. For all measurements, the values of σ are recorded just after changing γ to avoid the stress relaxation effect. This stress relaxation obeys a classical law $\sigma_R \propto t^{-m}$, where σ_R is the reduced stress (Figure 10). Typical values of m for c = 0.15 and 0.20 g/mL and T = −25 °C are m = 0.07, higher than generally found for chemically cross-linked networks[25,26] (m = 0.01). The values of E have been found to be independent of temperature for $T < T_{gel}$ as shown in Figure 11 for 0.15 g/mL PS*III. The temperature at which E drops is in good agreement with the temperature obtained by the ball-drop method.

The values of E for different concentrations of samples PS*II and PS*III are given in Table 3 and depicted in

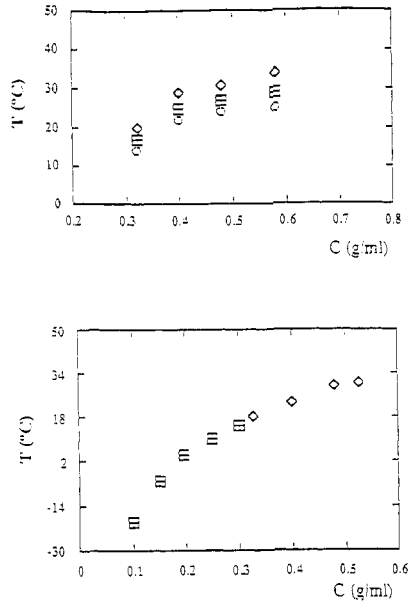

Figure 8. (a, Top) Phase diagrams obtained by DSC for sample PSD*1 corresponding to the maximum (■), end (◇), and onset (○) of the enthalpy peak. (b, Bottom) T_{gel} versus concentration for sample PSD*1: DSC (◇); ball-drop method (■).

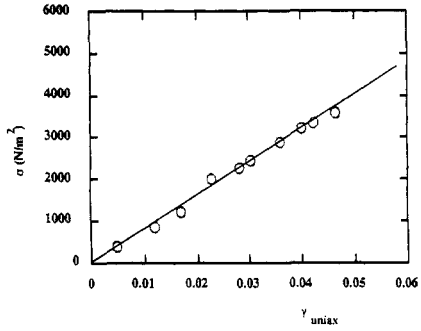

Figure 9. Plot of the stress σ vs the uniaxial deformation γ_{uniax} for the sample PS*III/CS_2 at T = −25 °C.

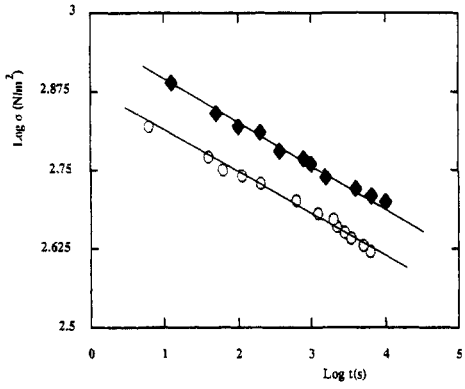

Figure 10. Variation of the stress as a function of time for sample PS*III at (○) 0.15 and (◆) 0.20 g/mL and T = −25 °C.

Figure 12. The whole set of data irrespective of the branch length can be fitted according to

$$E = 9.8 \times 10^5 c^{2.52} \quad (N/m^2) \quad \text{with } c \text{ in g/mL} \quad (11)$$

E. G' and G'' Measurements. An example of the frequency dependence of $G'(\omega)$ and $G''(\omega)$ is shown in Figure 13. For the lowest temperatures, corresponding to $-30 < T - T_{gel} < -10$ °C, the system exhibits a nearly elastic behavior, at least in the investigated frequency range, and therefore corresponds to the plateau modulus G_N. The variation of G_N with concentration is given in

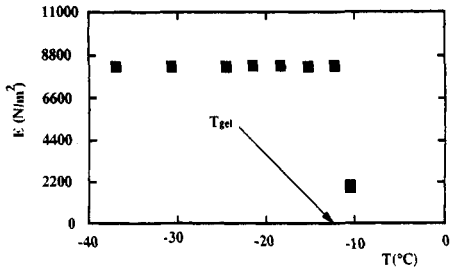

Figure 11. Young's modulus E vs temperature for sample PS*III at 0.15 g/mL.

Table 3. Variation of E and G_N with the Polymer Concentration

	c (g/mL)	E (N/m²)		c (g/mL)	G_N (N/m²)
PS*III	0.08	1686	PS*III	0.07	302
PS*III	0.1	2959	PS*III	0.09	588
PS*III	0.11	3763	PS*III	0.1	779
PS*II	0.14	6909	PS*III	0.16	2720
PS*III	0.174	11951	PS*III	0.2	4923
PS*III	0.21	19196	PS*III	0.27	10937
PS*II	0.24	26875			
PS*III	0.3	47160			

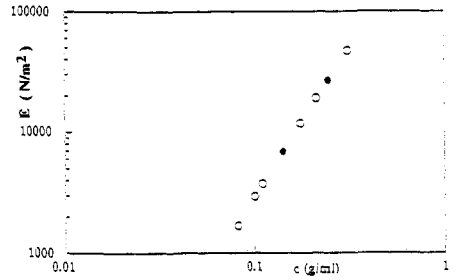

Figure 12. Logarithmic plots of the Young's modulus E in the gel phase vs polymer concentration for two different molecular weights: (●) PS*II; (○) PS*III.

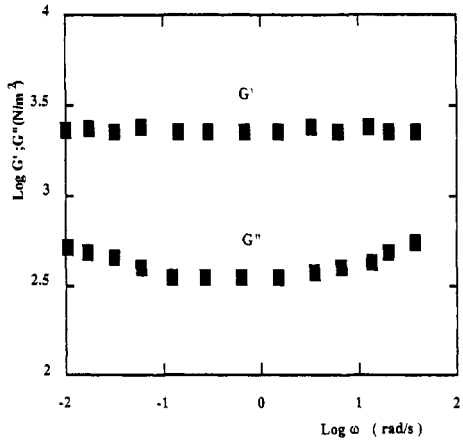

Figure 13. Examples of double-logarithmic plot of the storage $G'(\omega)$ and loss $G''(\omega)$ moduli vs the angular frequency for gel (PS*III/CS_2 at c = 0.15 g/mL and T = −25 °C).

Table 3 and is fitted according to

$$G_N = 3.56 \times 10^5 c^{2.66} \quad (N/m^2) \quad \text{with } c \text{ in g/mL} \quad (12)$$

The relation $G_N = E/3$ is approximately fulfilled within experimental error.

IV. Discussion and Conclusion

Three main facts emerge from our measurements:

(1) The sol–gel transition of aPS at a given concentration and molecular weight is shifted toward higher temperatures when passing from linear to star molecules.

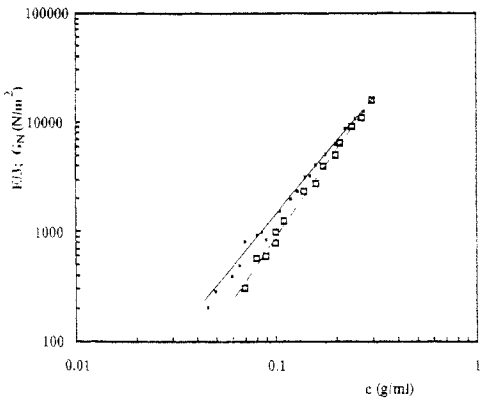

Figure 14. Variation of G_N and $E/3$ (□) as a function of polymer concentration at $T = -25$ °C (Table 3). Also reported are the values of G_N and $E/3$ for linear PS (■) with a different molecular weight.

(2) The sol–gel transition leads to a particular phenomenon which can be visually described versus temperature as follows: For $T < T_{gel}$ the solution is an optically clear translucid gel which can sustain a freely rolling steel ball on its surface. These properties persist even at lower temperatures in the swelling region of the PS–CS_2.

When the temperature is increased to $T = T_{gel}$ or several degrees above, the solution changes completely from its former behavior to a dark color with droplets of solvent on the surface, indicating a syneresis of the remaining pregel solutions. At this time the ball disappears in the solution and falls rapidly to the bottom of the sealed tube. The physical state encountered here needs to be more properly determined by other optical methods. The solution looks definitely different than a turbid or opalescent solution, which ascertains what is usually recognized for an LCST (–70 °C for CS_2). In fact, we never really observed a UCST or heated the concentrated solutions above 50 °C for safety reasons. Moreover, no precipitation or demixing process was observed, so our solutions were always stable for weeks.

(3) According to the classical relation ($E = 3G$) between the shear modulus and the Young's modulus, in an elastic incompressible material, the experimental values of $E/3$ for three-branch aPS are plotted in Figure 14 and both sets of experiments appear to be in good agreement. A unique scaling law for the variation of $E/3$ and G_N is obtained:

$$G_N = E/3 = 3.64 \times 10^5 c^{2.62} \quad (N/m^2) \quad \text{with } c \text{ in g/mL} \tag{13}$$

In the concentration range studied, the characteristic moduli are independent of the molecular weight. The results obtained for the different samples are given in Table 3.

The concentration dependence is slightly higher than found for linear aPS–CS_2 gels

$$G_N = E/3 = 2.6 \times 10^5 c^{2.3} \quad (N/m^2) \quad \text{with } c \text{ in g/mL} \tag{14}$$

but the absolute values are significantly lower (Figure 14) (note that the change in the exponent overcompensates the increase of the prefactor).

These two results point to the fact that chemical junctions in *p*-branched star molecules reduce the number of physical cross-links required for gelation at a given total molecular weight. The lower modulus observed at a given concentration for gels of branched star molecules as compared to linear molecules may also then be due to a reduced number of elastic chains for $p = 3$.

More experiments with stars with different numbers of branches in a larger range of lengths are needed to quantitatively interpret the changes in the phase diagram and in the gel moduli.

Acknowledgment. Special thanks are due to Mrs. J. François and M. G. Weill for helpful discussions of the results and to Mrs. M. Scheer for the DSC facilities.

References and Notes

(1) Tan, H. M.; Hiltner, A.; Moet, E.; Baer, E. *Macromolecules* **1983**, *16*, 28.
(2) Clark, J.; Wellinghoff, S. T.; Miller, W. G. *Polym. Prepr. (Am. Chem. Soc., Div. Polym. Chem.)* **1983**, *24* (2), 86.
(3) Gan, Y. S.; François, J.; Guenet, J. M.; Gauthier-Manuel, B.; Allain, C. *Makromol. Chem.* **1985**, *6*, 225.
(4) Gan, Y. S.; François, J.; Guenet, J. M. *Macromolecules* **1986**, *19*, 173.
(5) Bayer, R. F.; Baer, E.; Hiltner, A. *Macromolecules* **1985**, *18*, 427.
(6) Gan, Y. S.; Sarazin, D.; Guenet, J. M.; François, J. *Polymer* **1988**, *29*, 898.
(7) François, J.; Gan, Y. S.; Guenet, J. M. *Macromolecules* **1986**, *19*, 2755.
(8) Arnault, J.; Berghmans, H. *Polym. Commun.* **1987**, *28*, 268.
(9) Arnault, J.; Berghmans, H. In *Physical Networks*; Burchard, W., Ross-Murphy, S. B., Elsevier Applied Science: Amsterdam, 1988.
(10) Xie, X. M.; Tanioka, A.; Miyasaka, K. *Polymer* **1990**, *31*, 281.
(11) Izumi, Y.; Katano, S.; Funahashi, S.; Inoue, K. *Proc. Int. Conf. Neutron Scattering (ICNS 91)*, Oxford, UK, 1991.
(12) Izumi, Y.; Kanya, T.; Shibata, K.; Inoue, K. *Proc. Int. Conf. Neutron Scattering (ICNS 91)*, Oxford, UK, 1991.
(13) Lehsaini, N.; François, J.; Weill, G. *Macromolecules* **1993**, *26*, 7333.
(14) Lehsaini, N.; Muller,R.; Weill, G.; François, J., to be published in Polymer.
(15) Hertz, J.; Hert, M.; Strazielle, C. *Makromol. Chem.* **1972**, *160*, 213.
(16) Inoue, Y.; Konno, T. *Polym. J.* **1976**, *8*, 457.
(17) Takahashi, A.; Sakai, M.; Kato, T. *Polym. J.* **1980**, *12* (5), 335.
(18) Kuhn, W. *Kolloid Z.* **1936**, *76*, 258.
(19) Kuhn, W. *Kolloid Z.* **1939**, *87*, 3.
(20) Gramain, P.; Libeyre, R. *J. Appl. Polym. Sci.* **1970**, *14*, 383.
(21) Zimm, B. H.; Stockmayer, W. H. *J. Chem. Phys.* **1949**, *17*, 130.
(22) Stockmayer, W. H.; Fixman, M. *Ann. N.Y. Acad. Sci.* **1953**, *57*, 334.
(23) Zimm, B. H.; Kilb, R. W. *J. Polym. Sci.* **1959**, *37*, 19.
(24) Eldridge, J. E.; Ferry, J. D. *J. Phys. Chem.* **1954**, *58*, 992.
(25) Guenet, J. M.; Willwott, N. F. F.; Ellsmore, S. A. *Polym. Commun.* **1983**, *16*, 28.
(26) Candau, S. J.; Bastide, J.; Delsanti, M. *J. Polym. Sci.* **1982**, *44*, 27.